Electron Diffraction

Ultrafast Electron Crystallography of Surface Structural Dynamics with Atomic-Scale Resolution**

*Franco Vigliotti, Songye Chen, Chong-Yu Ruan, Vladimir A. Lobastov, and Ahmed H. Zewail**

Progress over the past two decades has made it possible to study atomic-scale femtosecond molecular dynamics in all phases of matter. The atomic-scale spatial resolution has been achieved with both X-ray and electron diffraction, and only recently has the combination of spatial and temporal resolution[1] been advanced successfully for studies of isolated chemical reactions by ultrafast electron diffraction[2,3] and bulk crystal phonons and melting[4–12] by X-ray diffraction. For surface structures and molecules on surfaces, ultrafast electron crystallography (UEC) is unique, and herein we demonstrate its potential for the direct determination of surface structural dynamics of crystalline solids (GaAs), following impulsive fs laser excitation. From the change of Bragg diffraction (shift, width, and intensity), we show, by direct inversion of the diffraction data, that *compression* and *expansion* of the atoms occur on the -0.01 Å to $+0.02$ Å scale, respectively, and that the transient temperature reaches its maximum value (1565 K) in 7 ps. The onset of structural change lags behind the rise in the temperature, demonstrating the evolution of non-equilibrium structures. These structural dynamics results are compared with those of nonthermal fs optical probing, and the agreement for the temperature response from the fluence dependence of the dielectric function is impressive.[13,14] The success in the direct observation of surface (monolayers) structural dynamics with combined ultrafast temporal and atomic-scale spatial resolutions promises many new applications of UEC.

GaAs is an ideal system to demonstrate this potential of UEC for surface studies, especially as its crystalline and semiconducting properties are well-quantified.[15] This has allowed a wide range of ultrafast optical experiments that vary from the probing of carrier properties[16] to electronic disordering or change in symmetry.[17] In addition to these optical studies, recent ultrafast X-ray experiments on GaAs revealed *bulk* lattice dynamics following fs laser excitation.[8] However, these ultrafast X-ray experiments could not probe the surface owing to the large penetration depth into the crystal by X-rays, typically up to several μm. On the other hand, optical techniques that probed the surface on the scale of a few nanometers could not directly determine the structure with atomic-scale resolution, but gave valuable information on the response of the dielectric function and lattice disordering.[13,14,17] The large scattering cross-section of electrons combined with ultrafast time resolution allows the bridging of this gap in addressing the dynamics of surface structures in real time.

The experiments were performed in the newly developed UEC apparatus,[18] briefly as follows (Figure 1). Under ultrahigh vacuum (10^{-10} Torr), and following surface characterization by low-energy electron diffraction and Auger spectroscopy, the sample was brought to the scattering position where beams of the laser-pulse excitation and electron-pulse probe intersected in space, with an adjustable time delay Δt (the zero of time was determined in situ). We followed a published procedure[19] to terminate semiinsulating GaAs (111) crystals by a monolayer of chlorine with a Cl atom atop each Ga atom, saturating the otherwise dangling bond of Ga. The surface retained its integrity throughout the experiments, as evidenced by the unchanged quality of the diffraction patterns (symmetry, spot profiles, and intensities)—see below. The crystal, placed on a goniometer with three degrees of freedom in translation and two axes of rotation, was positioned in space with a precision of 0.01° in rotation, and of 10 μm in translation. All experiments were carried out at room temperature.

[*] Dr. F. Vigliotti, S. Chen, Dr. C.-Y. Ruan, Dr. V. A. Lobastov, Prof. Dr. A. H. Zewail
Arthur Amos Noyes Laboratory of Chemical Physics
California Institute of Technology
Pasadena, CA 91125 (USA)
Fax: (+1) 626-792-8456
E-mail: zewail@caltech.edu

[**] This work was supported by the National Science Foundation. Some support was also provided by the Air Force Office of Scientific Research. F.V. acknowledges partial financial support from the Swiss National Science Foundation and S.C. a Millikan fellowship at Caltech. We thank Professor N. Lewis and L. Webb for functionalizing the silicon surface.

 DOI: 10.1002/ange.200453983

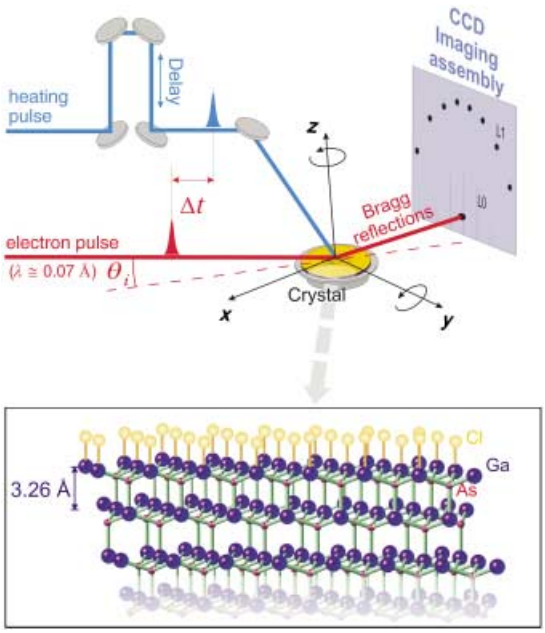

Figure 1. Concept of UEC and structure of the chlorine-terminated GaAs (111) crystal. The output of a Ti:Sa fs amplifier (120 fs, 800 nm, 2 mJ, 1 kHz) was frequency tripled to yield a beam at 266 nm (400 μJ, $<$300 fs, 1 kHz). This UV beam was brought to the scattering chamber to provide the initial heating pulse at $t=0$. A very small fraction of this beam was directed synchronously onto a back-illuminated Ag photocathode to generate the electron pulses. These electron pulses, after acceleration and focusing, were guided to the crystal, where they overlapped in space and time (delay Δt) with the heating pulse. Although electron pulses were made as short as 500 fs (see text), in this grazing incidence, the spatial extent decreases this resolution to tens of ps. However, because of the sensitivity achieved (20 s per frame), we were able to reduce the experimental temporal cross-correlation to 7 ps; with convolution and at the level of signal reported herein, we readily obtained a 1–2 ps response. This was made possible by reducing the spatial extent of the substrate to 400 μm by masking techniques (which will be described elsewhere in detail), resulting in a transit time of 4 ps. The sample, placed on a high-precision five-axis goniometer, was positioned to allow the electron beam to impinge at the chosen incidence angle ($\theta_i < 5°$), azimuthally along the $<112>$ direction. L0 and L1 refer to the zero-order and first-order Laue zones. The resulting diffraction patterns were recorded in the far field by an imaging CCD camera system. In the inset, the structure of the crystal is shown, with the bilayer spacing of 3.26 Å.

Femtosecond laser heating at $t=0$ initiated the dynamics, which were subsequently probed by an ultrashort packet of electrons of 30 keV ($\lambda_{deBroglie} \approx 0.07$ Å). The electrons impinged the surface at a small incidence angle ($\theta_i \approx 1°$) and at this grazing incidence, reflection high-energy electron-diffraction methods[20] are uniquely suited and have been used for studies of superheating with a temporal resolution of $\approx$100 ps.[21,22] The electron pulses were generated by a modified Williamson–Mourou[23] streak camera arrangement. In our UEC machine, we have obtained pulses of duration as short as $\approx$500 fs,[24–26] but for the grazing geometry of the experiment, the temporal cross-correlation was 7 ps. By controlling the arrival of the electron pulse (Δt in Figure 1), we can probe the structure prior to or following the heating pulse excitation. Structural changes were followed in real time by monitoring the Bragg reflections and rocking curves, as recorded by a CCD (charge-coupled device) imaging assembly capable of single electron detection.[2,3] Three features of the diffraction were followed as a function of time: the Bragg peak shift, width, and intensity.

Figure 2 presents a typical static diffraction image, which displays the very strong (0,0) and other Bragg reflections. Figure 2a shows a diffraction pattern, for which the incidence

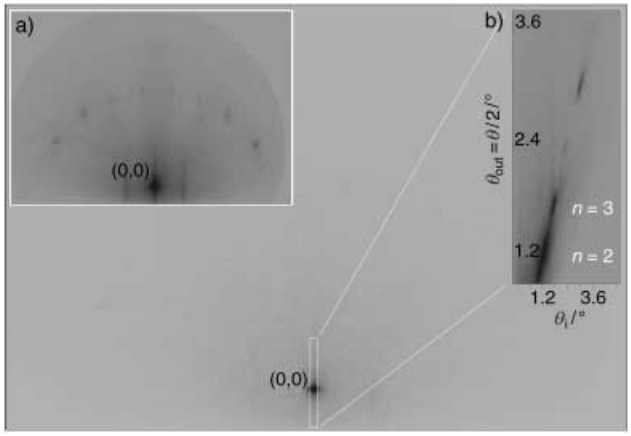

Figure 2. Static diffraction images of the crystal (111) surface obtained by the ultrashort electron pulses without time resolution. a) Diffraction image showing the intense (0,0) in-phase reflection, together with the streaks and spots in the Laue zones. b) Experimental rocking curve for the (0,0) reflection–(111) lattice planes. The periodicity allows the unequivocal identification of the Bragg reflections and gives the interlayer spacing (see text).

angle was tuned to reveal higher-order diffraction peaks, as well as diffraction streaks in the zero-order Laue zone. These and similar data allow the precise determination of the camera distance from the scattering position (170 $\pm$ 1 mm), by direct inversion of the angular separation between the streaks at low angles, or from the Bragg spots in the higher Laue zones. This inversion is direct because the lattice rods are separated in reciprocal space by an in-plane inverse distance of 3.14 Å^{-1} along the intersection with the Ewald sphere of radius $2\pi\lambda^{-1} = 90$ Å^{-1}. By gating the detection on the (0,0) Bragg spot and following the diffraction position as a function of the incidence angle, we also obtained the experimental rocking curve, which gives the GaAs lattice periodicity along the (111) direction ($n = 1, 2, \ldots$). This is shown in Figure 2b, where the incidence angle was varied over several degrees. The experimental periodicity in θ_i of 0.60° $\pm$ 0.02° is in quantitative agreement with the expected value of 0.61° obtained for the lattice bilayer spacing of 3.26 Å.

In the time-resolved experiment, depicted schematically in Figure 1, the excitation pulse at $t=0$ defines the initial temperature and structural change. In Figure 3, we follow the center position and intensity of the $n=2$ (0,0) Bragg spot as a function of time. We also monitor the width, as shown in Figure 3b. Figure 3a presents the change in the peak center position, which maps out the change in lattice spacing in the (111) direction. Results are shown for fluences of 9% and 45% of the experimentally determined 4.5 mJ cm^{-2} damage

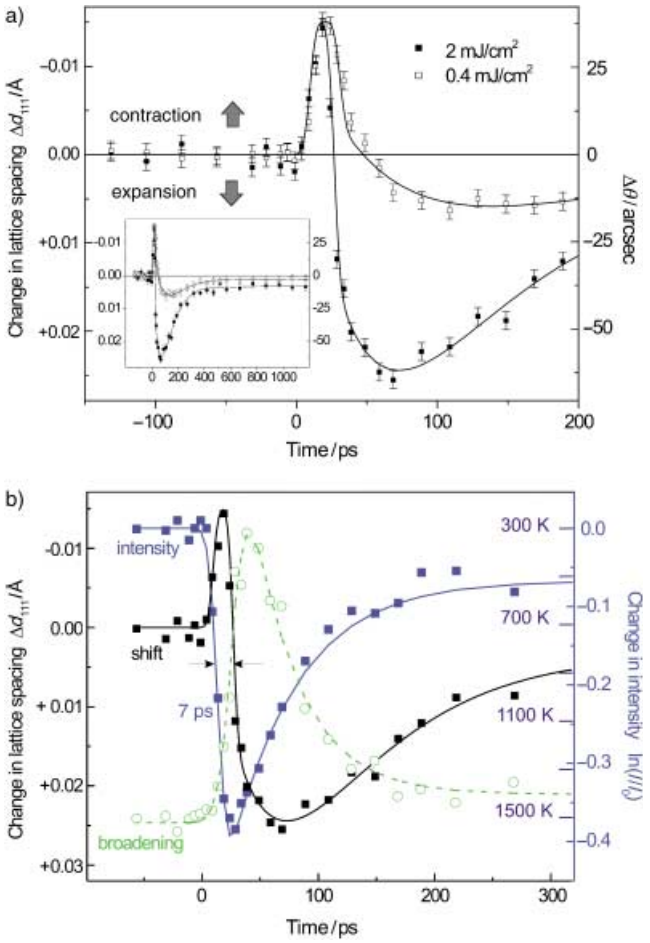

Figure 3. Time dependence of the Bragg reflection center position, intensity, and width, following the laser heating excitation at $t=0$. a) Center position of the Bragg spot as a function of time and fluence. The vertical axis on the right gives the angular deviation and the left axis shows the corresponding change in lattice spacing, perpendicular to the (111) surface plane. A contraction takes place at early times ($\Delta d<0$), followed by lattice expansion ($\Delta d>0$). The inset shows the evolution at long time. b) Comparison of the integrated intensity of the Bragg spot (temperature) with the change in lattice spacing for the data set obtained at 2 mJ cm^{-2}. The right axis gives the ratio of the time-dependent integrated intensity of the Bragg spot (I) to its counterpart at negative delay (I_o) on a logarithmic scale, from which the temperature scale is obtained. The lattice expansion is also shown with its scale on the left axis, together with the broadening of the Bragg spot, depicted by the dashed line. The apparent delay between the temperature rise and the lattice expansion is noted by the two arrows (see text).

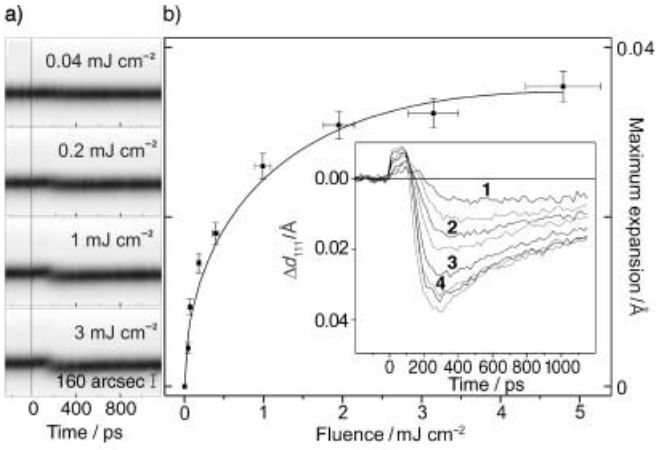

Figure 4. Fluence dependence of the structural dynamics. a) Experimental traces for a set of data at the indicated fluences. b) The amplitude at maximum change is shown as a function of excitation fluence. The time-dependence is displayed in the inset (**1**: 0.04, **2**: 0.2, **3**: 1, **4**: 3 mJ cm^{-2}). Notably, the temporal resolution is lower than that in Figure 3, because these fluence-dependent measurements were made without masking in order to explore the lowest possible range of fluences.

threshold at 266 nm. The angular deviation ($\Delta\theta$) of the Bragg spot directly gives the change in lattice spacing (Δd_{111}), from the relation $\Delta d_{111} = -\Delta\theta \cdot d_{111} \cdot \{2\sin(\theta/2)\}^{-1}$ (θ is the total scattering angle). A deviation to larger or smaller angles ($\Delta\theta>0$ or $\Delta\theta<0$) is therefore the signature of lattice contraction or expansion.

From the results shown in Figure 3a, it is evident that the top surface layers of the crystal immediately contract following excitation at $t=0$. The amplitude of this initial contraction is given for two fluences, but the complete fluence dependence is presented in Figure 4. After the initial contraction (-0.015 Å), the system expands to a maximum amplitude ($+0.025$ Å), which strongly depends on the fluence: the larger the fluence the more ample the expansion. The data also show that both the onset time and the velocity of the expansion ($\approx$ m s^{-1}) strongly depend on the fluence: expansion occurs earlier and faster at higher fluences. After reaching its maximum expansion, the system contracts again toward the original lattice spacing on a much longer time scale, beyond 50 ps, but a finite smaller expansion persists for at least several ns. Observations were also made for 800-nm fs excitation at various laser fluences and the behavior is similar, that is, an initial contraction, followed by an expansion and subsequent return toward the initial lattice spacing. This similarity in form, compared to that in the 266-nm experiment, indicates that the observed structural dynamics is not dominated by a charging of the surface by photoemission, as excitation at 800 nm and/or at low fluences results in a similar behavior.

The transient temperature is evident in the change in the diffraction-integrated intensity with time. This is presented in Figure 3b, for excitation at 45% of damage threshold (2 mJ cm^{-2}), by plotting the evolution of the integrated intensity of the Bragg spot as a function of time. Using the tabulated Debye–Waller factors for bulk GaAs,[27] and taking into account the two-dimensionality of the surface,[28] we obtained an initial temperature jump to 1565 ± 83 K. The system cools down on the timescale of a few hundred ps to reach $\approx$510 K after 1 ns. The initial temperature jump has a rise time of 7 ps (10 ps before deconvolution), in perfect agreement with results from fs optical studies of the dielectric function.[13,14] Moreover, the maximum temperature reported above is close to the value (1300–1500 K) extrapolated from these optical studies at corresponding fluence. For the lower

fluence regime (0.4 mJ cm^{-2}) presented in Figure 3a, we find a temperature jump to 420 ± 18 K, with a decay leveling off at 320 ± 5 K after 1 ns. In this case too, the rise time and the maximum temperature are consistent with the optical study.

The evolution of the lattice expansion and that of the temperature are juxtaposed in Figure 3b, together with the width. Strikingly, the temperature evolution precedes the lattice expansion, and we measured a delay of 15 ps between the rise in temperature and the structural expansion. This lag in structural expansion provides direct evidence for the proposed delayed lattice changes following an impulsive initial temperature.[13,14] We note that the temperature jump to 1565 ± 83 K is similar to (or even exceeds) the 1513 K melting point,[15] whereas the excitation fluence is only half of the damage threshold. However, as evident from Figure 3b, the peak temperature does not persist for a long time and the system does not lose its crystalline structure.

The lagged structural change reaches its maximum expansion of $+0.025$ Å at a temperature of ≈ 1000 K (Figure 3b). This lattice expansion in the nm-scale structure may now be compared with the expansion in bulk GaAs. From the linear expansion coefficient of bulk crystals,[15] a temperature of 1000 K would correspond to a linear lattice expansion of 0.013 Å, and this value differs by a factor of 2 from our experimental value of 0.025 ± 0.001 Å. At much longer times (≈ 1 ns), when the change in expansion levels off, a temperature of 510 K would correspond to a linear expansion of 0.0038 Å, and our experimental value is 0.0032 ± 0.0005 Å (Figure 3b). This temporal decrease in the disparity in spacing is indicative of the change in surface to bulk-type behavior. From modeling of strain propagation in X-ray studies, a 0.0082-Å surface strain amplitude was inferred for GaAs.[8] Our measurements indicate a larger deformation (by a factor of 3).

Because of their small incidence angle, the probing electrons have a very small penetration depth (a few Å for 30-keV electrons at $\theta_i \approx 1°$) and thus probe only the very top surface layers of the crystal; in the geometry of our experiment, the excitation pulse (30° incidence angle) has a vertical penetration depth also of nm scale (3.5 nm at 266 nm). These small and comparable penetration depths for the photons and electrons provide a unique condition for monitoring the local structural dynamics of these surface layers. In X-ray experiments, a heating pulse typically has an absorption length of 0.3 μm, and the probing X-ray pulse has a μm-scale penetration depth. Such scales require consideration of strain propagation in the bulk and over the μm(s) length.[8] Clearly, direct probing of the surface motions of atoms is critical to the understanding of the surface initial dynamics and to the connection to bulk propagation at different temperatures (fluences). The effect of fluence on structural changes is mapped out in Figure 4a, and representative examples of experimental traces that follow the time-dependent Bragg reflection are shown in Figure 4b.

Additional experiments were carried out on silicon to isolate the effect of chlorination and to test the generality of the approach and the scope of application. Both chlorinated and non-chlorinated silicon (111) surfaces were subjected to the same experimental conditions (excitation wavelength and fluence). Similar behavior to that of GaAs was found—whereas hydrogen-terminated silicon did not present noticeable surface contraction preceding the expansion, the chlorinated surface showed a prompt contraction, which precedes the expansion. The overall phase of the signal in Figure 3 depends on the overlap at the mask (Figure 1, caption) and it is possible that optical phonon generation at $t = 0$ contributes to the observed scattering. It should be noted that the phase corresponding to the expansion is unequivocally established and confirmed by the temporal evolutions of the temperature and structural dynamics at different fluences. Several mechanisms were considered for the striking nature of the contraction, as will be described in detail elsewhere. However, the observations with chlorine are consistent with a potential-driven change at the earliest times, prior to coherent acoustic phonon generation.

A general structural-dynamics picture now emerges from the observations of the structure changes and the timescales of the motion (Figure 3b), and from the observations on silicon surfaces. In the nonthermal regime,[13] the initial fs transient excitation, which creates the electron-hole pairs, distorts the potential, and structural changes occur on the ultrashort timescale by this deformation prior to significant motion in the lattice (phonons), as experimentally verified above. This highly non-equilibrium state of the solid is followed by energy dissipation and redistribution, which ultimately lead to expansion of the lattice and restructuring at longer times. With this in mind, only an expansion of the surface atoms would be expected, contrary to the *contraction* and *expansion* observed in the studies reported herein. However, for the chlorine-terminated surface, the large electronegativity shifts the electronic charge distribution towards the chlorine (ionic potential). The ensuing Coulombic interaction with the underlying layers contracts the interatomic layers, as observed in the early-time ultrafast rise of the contraction (Figure 3a), and on this timescale, the dynamics is driven by the potential change. Along with the observations made in the case of silicon and supporting this proposed mechanism for contraction, we note that atomic chlorine chemisorbed on GaAs was found to be an electron acceptor.[29]

Following the contraction, expansion proceeds on a similar timescale. Through Auger processes (at a density of $\approx 10^{21}$ cm^{-3}), which take place in a few ps, the carrier density decreases, but the total electronic energy remains unchanged.[13,30,31] The drop in the Coulombic potential along with electron–phonon coupling now drives the system in a reversed motion toward expansion (Figure 3a). The expansion of the lattice requires 7 ps to define surface-layer temperature and this is evident in the rise of the intensity profile (Figure 3b); only after this rise can we define the temperature acquired through electron–phonon coupling. The structural change (expansion) follows the temperature rise, but after the apparent delay of 15 ps, reaching its maximum of $+0.025$ Å expansion at yet longer time. This thermal expansion in the (111) direction must be due to anharmonicity of lattice vibrations. Remarkably, the width of the Bragg spot reaches its maximum before the peak of structural lattice expansion. Lattice dynamics is first driven by

coherent collective phonons followed by the isotropic expansion that ensues when anharmonicity becomes effective. This nascent lattice expansion must first overcome the persisting contraction (Figure 3a). From our data, we obtained an onset for the expansion of ≈ 5 ps after the temperature has risen to half of its maximum and an additional delay of ≈ 10 ps to overcome the initial contraction. It should be noted that this picture of structural dynamics is robust at lower fluences (Figure 4). However, in the lower fluence regime, the initial temperature is decreased, electron–phonon coupling dominates, and diffusive processes become pronounced at longer times.

The return to the original structure is observed in the decrease in Δd_{111}, from $+0.025$ to $+0.003$ Å, but this restructuring takes place on a much longer timescale (Figure 3). We note that diffusive processes must begin beyond 50 ps, as up to this time Δd_{111} continues to increase—cooling down the surface by diffusion leads to a decrease in Δd_{111}. Thus, the structure at the expanded value of $\Delta d_{111} = 0.025$ Å is vibrationally in a non-equilibrium state of collective modes, which cools down by energy redistribution and diffusion at longer times. Theoretical calculations of the heat diffusion using the known thermal properties of GaAs (heat capacity and thermal conductivity[15]) gave a good match to the temperature behavior from the point of leveling off shown in Figure 3b.

The above results show the new dimensions of ultrafast electron crystallography at time, length, and sensitivity scales ideally suited for atomic-scale structural dynamics of surfaces and interfaces. This is achieved because of the ability to directly determine—from the diffraction periodicity and changes with time—the evolution of atomic spacings (Bragg peak positions), transient temperatures (Bragg integrated intensity), and the involvement of coherent lattice vibrations (Bragg peak width). The timescales for the non-equilibrium surface structures, and restructuring at longer times, are critical for understanding the surface phenomena and for propagation in bulk materials. We believe that UEC is now poised for many applications in this general area of surface science and nanometer-scale materials, and macromolecular structures.[32]

Received: February 10, 2004 [Z53983]
Published Online: March 23, 2004

Keywords: electron diffraction · structural dynamics · surface chemistry · X-ray diffraction

[1] A. Rousse, C. Rischel, J.-C. Gauthier, *Rev. Mod. Phys.* **2001**, *73*, 17–31.
[2] H. Ihee, V. A. Lobastov, U. Gomez, B. M. Goodson, R. Srinivasan, C.-Y. Ruan, A. H. Zewail, *Science* **2001**, *291*, 458–462.
[3] R. Srinivasan, V. A. Lobastov, C.-Y. Ruan, A. H. Zewail, *Helvetica Chimica Acta* **2003**, *86*, 1763–1838.
[4] K. Sokolowski-Tinten, C. Blome, C. Dietrich, A. Tarasevitch, M. Horn-von-Hoegen, D. von der Linde, A. Cavalleri, J. Squier, M. Kammler, *Phys. Rev. Lett.* **2001**, *87*, 225701.
[5] K. Sokolowski-Tinten, C. Blome, J. Blums, A. Cavalleri, C. Dietrich, A. Tarasevitch, I. Uschmann, E. Foster, M. Kammler, M. Horn-von-Hoegen, D. von der Linde, *Nature* **2003**, *422*, 287–289.
[6] A. M. Lindenberg, I. Kang, S. L. Johnson, T. Missalla, P. A. Heimann, Z. Chang, J. Larsson, P. H. Bucksbaum, H. C. Kapteyn, H. A. Padmore, R. W. Lee, J. S. Wark, R. W. Falcone, *Phys. Rev. Lett.* **2000**, *84*, 111–114.
[7] D. A. Reis, M. F. DeCamp, P. H. Bucksbaum, R. Clarke, E. Dufresne, M. Hertlein, R. Merlin, R. Walcone, H. Kapteyn, M. M. Murnane, J. Larsson, T. Missalla, J. S. Wark, *Phys. Rev. Lett.* **2001**, *86*, 3072–3075.
[8] C. Rose-Petruck, R. Jimenez, T. Guo, A. Cavalleri, C. W. Siders, F. Ráksi, J. A. Squier, B. C. Walker, K. R. Wilson, C. P. J. Barty, *Nature* **1999**, *398*, 310–312.
[9] C. W. Siders, A. Cavalleri, K. Sokolovski-Tinten, C. Tóth, T. Guo, M. Kammler, M. Horn von Hoegen, K. R. Wilson, D. von der Linde, C. P. J. Barty, *Science* **1999**, *286*, 1340–1342.
[10] A. H. Chin, R. W. Schoenlein, T. E. Glover, P. Balling, W. P. Leemans, C. V. Shank, *Phys. Rev. Lett.* **1999**, *83*, 336–339.
[11] C. Rischel, A. Rousse, I. Uschmann, P.-A. Albouy, J. P. Geindre, P. Audebert, J.-C. Gauthier, E. Förster, J.-L. Martin, A. Antonetti, *Nature* **1997**, *390*, 490–492.
[12] A. Rousse, C. Rischel, S. Fourmaux, I. Uschmann, S. Sebban, G. Grillon, P. Balcou, E. Förster, J. P. Geindre, P. Audebert, J.-C. Gauthier, D. Hulin, *Nature* **2001**, *410*, 65–68.
[13] S. K. Sundaram, E. Mazur, *Nat. Mater.* **2002**, *1*, 217–223.
[14] L. Huang, J. P. Callan, E. N. Glezer, E. Mazur, *Phys. Rev. Lett.* **1998**, *80*, 185–188.
[15] J. S. Blakemore, *J. Appl. Phys.* **1981**, *53*, R123-R181.
[16] J. Shah, *Ultrafast Spectroscopy of Semiconductors and Semiconductor Nanostructures*, Springer, Berlin, **1996**.
[17] P. Saeta, J.-K. Wang, Y. Siegal, N. Bloembergen, E. Mazur, *Phys. Rev. Lett.* **1991**, *67*, 1023–1026.
[18] C.-Y. Ruan, F. Vigliotti, V. A. Lobastov, S. Chen, A. H. Zewail, *Proc. Natl. Acad. Sci. USA* **2004**, *101*, 1123–1128.
[19] Z. H. Lu, T. Tyliszczak, A. P. Hitchcock, *Phys. Rev. B* **1995**, *58*, 13820–13823.
[20] Z. L. Wang, *Reflected Electron Microscopy and Spectroscopy for Surface Analysis*, Cambridge University Press, Cambridge, **1996**.
[21] M. Aeschlimann, E. Hull, C. A. Schmuttenmaer, J. Cao, L. G. Jahn, Y. Gao, H. E. Elsayed-Ali, D. A. Mantell, M. Scheinfein, *Rev. Sci. Instrum.* **1995**, *66*, 1000–1009.
[22] B. Lin, H. E. Elsayed-Ali, *Surf. Sci.* **2002**, *498*, 275–284.
[23] S. Williamson, G. A. Mourou, J. C. M. Li, *Phys. Rev. Lett.* **1984**, *52*, 2364–2367.
[24] V. A. Lobastov, R. Srinivasan, F. Vigliotti, C.-Y. Ruan, J. S. Feenstra, S. Chen, S. T. Park, S. Xu, A. H. Zewail in *Springer Series in Optical Sciences* (Eds.: F. Krausz, G. Korn, P. Corkum, I. Walmsley), Springer, **2003**, p. 413–429.
[25] J. Cao, Z. Hao, H. Park, C. Tao, D. Kau, L. Blaszczyk, *Appl. Phys. Lett.* **2003**, *83*, 1044–1046.
[26] B. J. Siwick, J. R. Dwyer, R. E. Jordan, R. J. D. Miller, *Science* **2003**, *302*, 1382–1385.
[27] J. F. Vetelino, S. P. Gaur, S. S. Mitra, *Phys. Rev. B* **1972**, *5*, 2360–2366.
[28] L. J. Clarke, *Surface Crystallography*, Wiley, New York, **1997**.
[29] D. Troost, L. Koenders, L.-Y. Fan, W. Mönch, *J. Vac. Sci. Technol. B* **1987**, *5*, 1119–1124.
[30] M. C. Downer, C. V. Shank, *Phys. Rev. Lett.* **1986**, *56*, 761–764.
[31] T. Sjodin, H. Petek, H.-L. Dai, *Phys. Rev. Lett.* **1998**, *81*, 5664–5667.
[32] C.-Y. Ruan, V. A. Lobastov, F. Vigliotti, S. Chen, A. H. Zewail, *Science*, in press.

Please note: Minor changes have been made to this manuscript since its publication in *Angewandte* Early View. The Editor.

